

# Laser Milling of Metallic and Non-Metallic Substrates in the Nanosecond Regime with Q-Switched Diode Pumped Solid State Lasers

Paul M Harrison, Matthew Henry, Ian Henderson, Michael Brownell  
Powerlase Ltd, Imperial House, Link 10, Napier Way, Crawley, West Sussex, UK, RH10 9RA

## ABSTRACT

Laser milling of a variety of substrates is investigated with the intention of achieving high quality material removal to create three-dimensional shapes in the material. A high power Q-switched Diode Pumped Solid State Nd:YAG Laser at 1064nm is used in all cases. Materials investigated include Nickel Superalloys, Thermal Barrier Coatings, Steels, Tungsten Carbide and Polycrystalline Diamond. Multi-layer substrates are also considered. The effects of laser intensity, plasma formation, pulse duration, material properties, and resulting removal rate, recast and surface finish are explored for this process. This paper defines the findings of this study within the context of commercial imperatives.

**Keywords:** laser, q-switched, diode pumped, ablation, nanosecond, milling, modelling, stainless steel, tungsten carbide.

## 1. INTRODUCTION

Nd:YAG Flash Lamp Pumped Solid State Lasers (FPSSLs) have been widely used in industry for over twenty years, but it is only relatively recently that industrially rugged Diode Pumped Solid State Lasers (DPSSLs) have become available<sup>6,7</sup>. Q-switched DPSSLs are now available at comparable average powers to pulsed FPSSLs and offer pulse durations in the nanosecond regime at kHz repetition rates. Much higher energy intensities are possible than with more conventional FPSSLs, which typically operate at a few hundred Hz and have pulse durations in the millisecond regime. The nanosecond-kHz regime of operation has the potential for much improved processing; since short pulses can diminish thermal effects and the higher fluences improve material coupling and process efficiency. The combination of good beam quality, high efficiency, rugged construction and long diode lifetime makes DPSSLs a very attractive option to industry seeking an advantage in cutting edge manufacturing on both the macro and micro scale.

This paper is a comparative study of laser milling, an emerging process enabled by the latest state-of-the-art Q-switched DPSSLs. This is a process by which complex 3D shapes can be made in materials, which are traditionally difficult to machine, such as stainless steel and aerospace alloys. The aim of the study is to develop a simple model of the laser milling process that can be used to predict the best starting point for practical work, thus accelerating future laser milling trials in different materials. This model is developed from established relationships and validated with empirical data.

## 2. MODELLING OF PULSED LASER ABLATION

When a high power laser beam strikes a target surface, there are four main phenomena that occur<sup>1,5</sup>. This applies to pulsed laser beams on the assumption that the process starts again every time a pulse hits the target. The process is described as follows:

*Absorption and Heating.* Part of the incident laser pulse is reflected and the rest is absorbed by the target.

*Melting.* The heat energy penetrates into the target by thermal conduction. In the case that the laser pulse has sufficient length and irradiance, the target will firstly melt and then start to vaporize.

*Vaporization.* After the vaporization temperature has been reached, an equilibrium condition is achieved where material is continually removed from the target as a vapour, and the result is the drilling of a hole into the target.

*Plasma Production.* If the laser pulse irradiance is high enough, absorption in the vaporised material leads to a hot opaque plasma<sup>1,3</sup>. This plasma absorbs the incoming laser beam and prevents further vaporization. This effect is also known as LSA (Laser Supported Absorption) or plasma blocking, and generally starts to occur<sup>1</sup> at laser irradiances greater than  $1.5 \times 10^8 \text{ W/cm}^2$ .

### 2.1. Assumptions made for the specific model of pulsed laser ablation

A specific model of pulsed laser ablation has been developed by making the following assumptions:

- The ‘‘Absorption and Heating’’ phase will be considered to be instantaneous. For the purposes of this study the absorbed energy is transformed instantaneously into heat energy at the surface of the target.
- The incident irradiance during this study will have an upper limit of  $3 \times 10^8 \text{ W/cm}^2$ , which is just above the LSA limit. It is also assumed that for the duration of the pulse the incident light does not interact with the vapour coming from the target. This means that for this study the ‘‘Plasma Production’’ phase of the model described in Section 2 can be ignored.
- To simplify the mathematics of the model two assumption have been made – firstly that the irradiance is constant for the duration of the pulse, and secondly that the irradiance is constant over the area of the focal spot.
- The equations shown in Figure 1 are based on the assumption that heat flow in the target material is one-dimensional and all of the absorbed laser energy is used in the vaporization process. This assumption is acceptable if the vaporization speed is similar to or faster than the rate of conduction<sup>2</sup>.
- Secondary effects of the vaporised material, such as the change in pressure near the target affecting the vaporisation temperature of the target will not be included in this study. Ambient pressure is assumed in all cases.
- The only removal mechanism that will be considered for this study is vaporization. Other removal methods, such as material removal in the form of liquid droplets are not considered.
- Average heating effects that raise the ambient temperature of the target material are not considered. The nanosecond pulse widths used in this study have high irradiances and low fluence so the heating effects are low.

### 2.2. The specific model of pulsed laser ablation

The specific model of pulsed laser ablation can be described as a series of laser pulses that can each be modelled in 2 stages described below and illustrated in Figure 2.

*Stage 1 – Melting.* This corresponds to the melting stage of the original model. The formula to calculate the time to reach the vaporization temperature,  $t_B$ , is given in Figure 1<sup>1</sup>.

*Stage 2 – Material Removal.* This corresponds to the Vaporization stage of the original model. The vaporizing surface retreats at a steady rate,  $v_B$ , perpendicular to the surface of the target until the end of the laser pulse and the formula to calculate  $v_B$  is shown in Figure 1. Combined with the focal spot size and the time available for this stage (which is the remainder of the pulse after the Melting stage,  $t_R$ ), the volume removed by each pulse can be modelled and an overall removal rate can be calculated.

<p><math>t_B</math>, the time to vaporization [s], is given by :</p> $t_B = \frac{\pi K \rho c (T_B - T_0)^2}{4 F^2}$ <p><math>v_B</math>, the vaporization speed [m/s], is given by</p> $v_B = \frac{F}{\rho [L + c (T_B - T_0)]}$	<p>Where :</p> <p><math>K</math> = Thermal conductivity [W/m °K]  <math>\rho</math> = Density [kg/m<sup>3</sup>]  <math>c</math> = Heat capacity [J/kg °K]  <math>T_B</math> = Vaporization temperature [°K]  <math>T_0</math> = Ambient temperature [°K]  <math>F</math> = Absorbed irradiance [W/cm<sup>2</sup>]  <math>L</math> = Specific latent heat of Vaporization [kJ/kg]</p>
---	---

Fig. 1. Formulae to calculate Time to Vaporization and Vaporization Speed

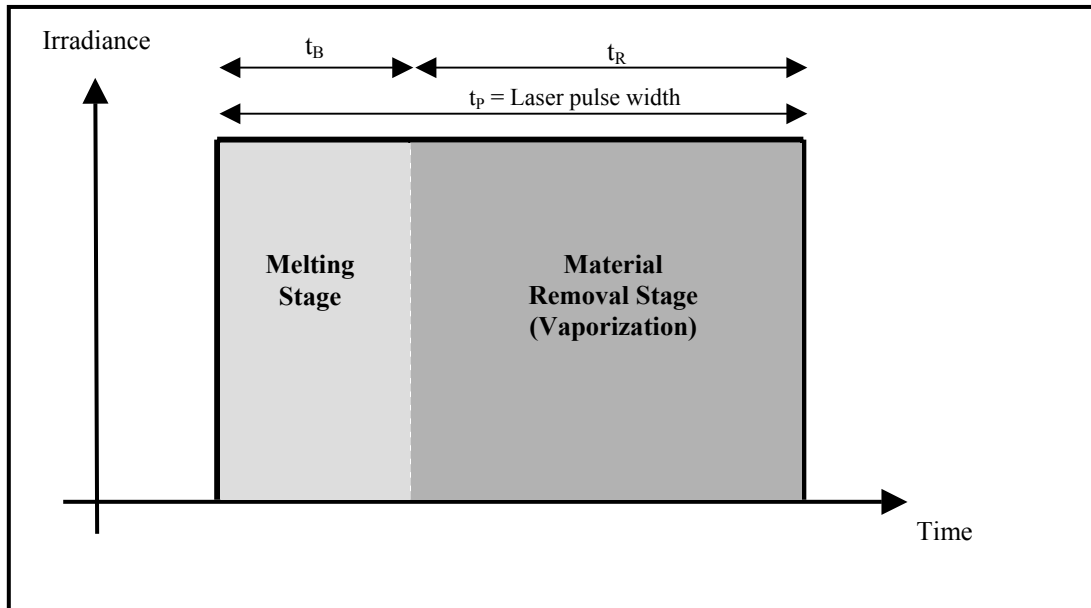


Fig. 2. Specific model of a single laser pulse

### 2.3. Implementation of the specific model

In order to implement the model, two sets of information are required. Firstly some material-specific parameters are required ( $K$ ,  $\rho$ ,  $c$ ,  $T_B$  and  $L$ ), and secondly a set of laser pulse parameters are needed ( $t_p$ ,  $F$ ,  $T_0$  and focal spot diameter). Measured laser pulse parameters are used in the model to allow easy comparison with experimental results.

The first part of the modelling process is to determine the absorbed irradiance, which is based on the incident irradiance and the reflectance of the target. The next step is to calculate the value of  $t_B$ , which also determines  $t_R$ , the removal time of the pulse. Subsequently  $v_B$ , the vaporization speed, is determined which allows the volume removed per pulse to be modelled. Finally incorporating the laser repetition rate allows the overall removal rate to be calculated. The modelling results are presented and discussed in Section 3.

## 3. COMPARISON OF MODELLED AND EXPERIMENTAL RESULTS

### 3.1. Experimental

For all of the laser milling tests a Starlase AO2 Nd:YAG Q-Switched DPSS laser was used at the fundamental wavelength 1064nm. This laser offers average powers up to 220W at a range of repetition rates and pulse durations between 3 to 50kHz and 20 to 200ns respectively. The output beam is attenuated using a proprietary unit. The output beam is collimated with a Galilean telescope and directed into a ScanLab HurryScan25 galvanometric scanner. During the course of the tests the scanner was fitted with an 80mm f-theta telecentric objective lens with a working target area of 25x25mm. All of the processing work was performed in air at standard atmospheric conditions and no gas assist was used.

Samples were analysed using a Nikon LM1500 optical microscope with a PC interface via a 12M pixel camera into Lucia G software. This software allowed microscopic measurements to be made against a Nikon standard. Depth measurements were made using a Mituyoto dial gauge.

The Starlase range of lasers is manufactured exclusively by Powerlase Ltd, UK.

### 3.2. Test Sequence

In order to verify the specific model of the pulsed laser ablation process, a set of test cases were identified that would be used to provide experimental volume removal data for comparison with the predictions of the model. Four test cases were chosen using two contrasting materials, stainless steel grade 316 and tungsten carbide (which is used as a backing material with Polycrystalline Diamond to make PCD cutting tools). The material properties of these two materials are shown in Table 1, and it shows that the two materials have very different characteristics, which is useful in showing that the model is working correctly.

Parameter	Units	Stainless Steel 316	Tungsten Carbide
K	W/m K	16.3	164
$\rho$	kg/m <sup>3</sup>	8000	19300
c	J/kg °C	500	140
T <sub>B</sub>	°C	3000	5930
L	kJ/kg	6500	4020

Table 1. Material properties for stainless steel 316 and tungsten carbide.

A set of test cases for this study were chosen which are shown in Table 2. These test cases had the aim of establishing the material removal rate within a range of irradiance levels for comparison. For each of the test cases, a set of trials were performed as described in Section 3.2.1

Test Case	Material	Laser Repetition Rate [kHz]	Irradiance Range [W/cm <sup>2</sup> ]
1	Stainless steel 316	30	$6.3 \times 10^7$ to $2.5 \times 10^8$
2	Stainless steel 316	50	$2.4 \times 10^7$ to $9.5 \times 10^7$
3	Tungsten carbide	30	$7.7 \times 10^7$ to $3.1 \times 10^8$
4	Tungsten carbide	50	$2.7 \times 10^7$ to $1.1 \times 10^8$

Table 2. Study sequence test cases

In parallel to the trials, the process was modelled using the “Specific Model of Pulsed Laser Ablation” described in Section 2.2. using the experimental values for irradiance, pulse width, repetition rate and focal spot size.

The results of the modelling work are show in Section 3.3. The aim was firstly to show for each test case how the laser pulses are divided into Melting and Material Removal stages and then to calculate a removal rate.

#### 3.2.1. Practical ablation trials

For each test case a set of four ablation trials were performed<sup>4</sup> where each trial aimed to ablate a 2x2mm square into the material. Most conditions were kept constant (focal spot size, laser repetition rate, scanner settings) whilst the irradiance was varied through the trials in equal steps between 25% through to 100% of maximum (which was altered via the laser power attenuator) as shown in Figure 3. The depth of the ablated region was then measured, and the total volume removed and overall removal rate calculated. Other properties of the ablated region were noted such as surface debris, sidewall taper angle and base roughness.

Each trial lasted approximately 30 seconds. It was found that trials of this length produced ablation depths up to 800µm (which is within the Rayleigh range of the objective lens) and were easy to measure. Each trial was accurately timed in order to calculate the volume removal rate.

The laser repetition rate and pulse width for the Starlase AO2 laser are interdependent. By setting the repetition rate and adjusting the irradiance (which can be achieved by using the attenuator to control the output power) the effect of pulse width alone can be examined. During the experimental tests the laser was operated mainly between 30 to 50kHz. Figure 3 shows the irradiance range of the laser at these repetition rates for different attenuator settings.

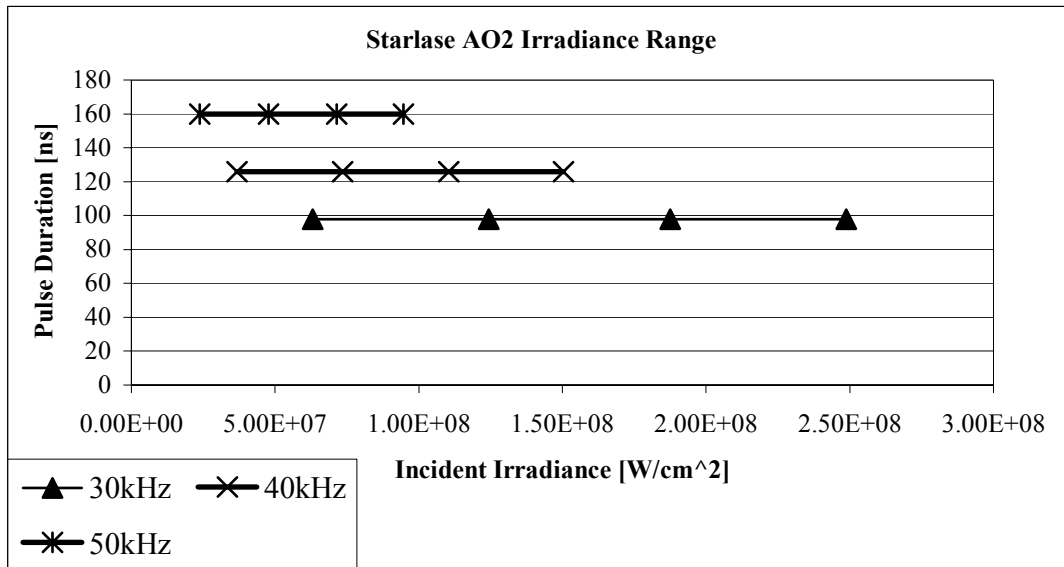


Fig. 3. Starlase AO2 irradiance range at focus for varying laser repetition rate when using an 80mm objective scanner lens

### 3.3. Analysis of results obtained using the specific model

Figures 4 to 7 show the results obtained from the specific model using the same initial conditions (material and laser pulse characteristics) as for the experimental work. Each figure shows a different test case, and shows for each of the four trials of that test case how a single pulse is divided into the Melting and Removal stages.

Referring to Figure 1, it can be seen that for a given material the vaporization time,  $t_B$ , is dependant only on the absorbed irradiance, because for this study all the other values are considered constant for that material. This means that for any absorbed irradiance described in Figure 3, stainless steel reaches its vaporisation temperature 26.75 times quicker than for tungsten carbide. This can be seen by comparing the Melting Stage times shown in Figure 4 with those shown in Figure 6, and comparing the Melting Stage times shown in Figure 5 with Figure 7.

In a similar fashion, referring again to Figure 1, for a given material the vaporization speed is also dependant only on absorbed irradiance because for this study all the other values are considered constant for that material. This means that during the Removal Stage, stainless steel is removed 1.3 times faster than for tungsten carbide. The lightly shaded area of each pulse shown in Figures 4 to 7 is an indication of how much material is removed per pulse since the vaporization speed,  $v_B$ , is proportional to irradiance.

Comparing the pulse analysis of corresponding trials of stainless steel at 30kHz and 50kHz (Test Cases 1 and 2), it can be seen that at 30kHz (where the pulse duration is shorter and the available incident irradiance higher) the duration of the Melting Stage is much shorter than for 50kHz. Although at 30kHz the pulse duration is shorter the amount removed per pulse (indicated by the area of the Material Removal stage) is slightly larger than for 50kHz. However the overall removal rate for 50kHz is higher because there are more pulses per second.

When comparing the pulse analysis of corresponding trials of tungsten carbide (Test Cases 3 and 4), it can be seen that at 50kHz only the trial at maximum available irradiance has a Removal Stage – for the other three pulses the target never reaches the vaporization temperature within the pulse duration so there is no material removal. On the other hand, at 30kHz almost every trial has a significant Removal Stage which means that the material removal rates at 30kHz are much more tolerant to changes in irradiance.

The removal rate prediction of this model is that for stainless steel the removal rate will be greatest with this laser operating at 50kHz, and for tungsten carbide the removal rate will be greatest when running at 30kHz.

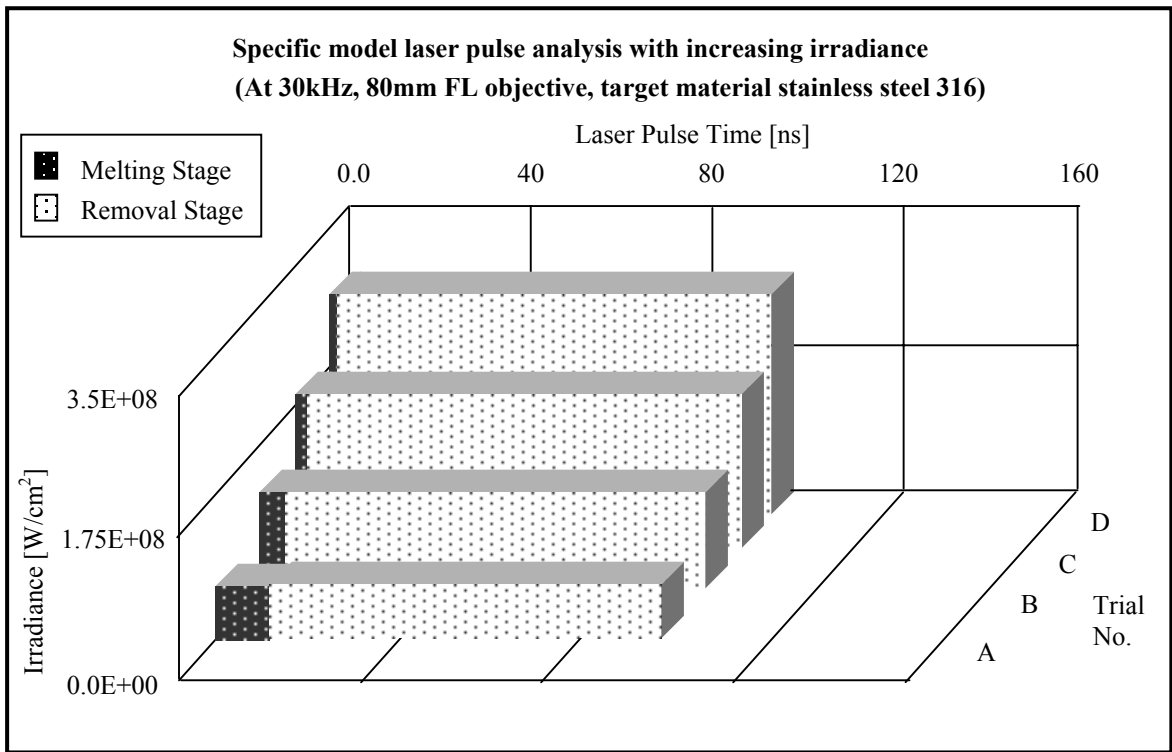


Figure 4 : Analysis of irradiance effects on Melting Stage for Test Case 1

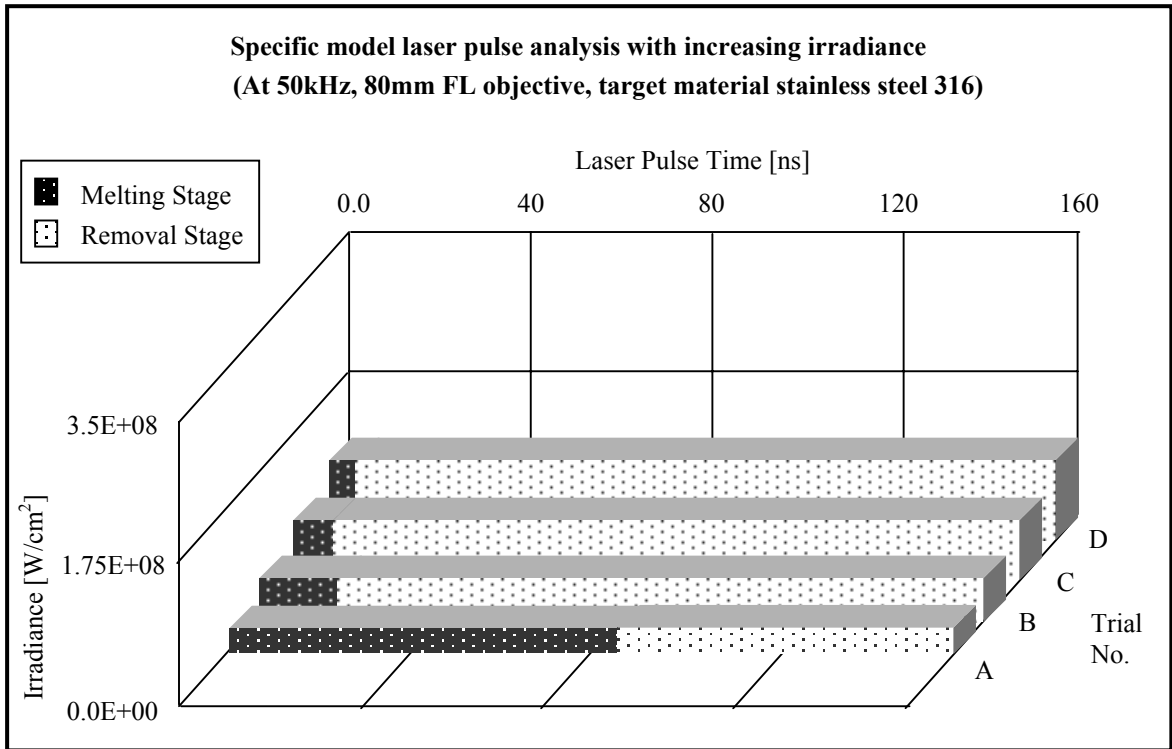


Figure 5 : Analysis of irradiance effects on Melting Stage for Test Case 2

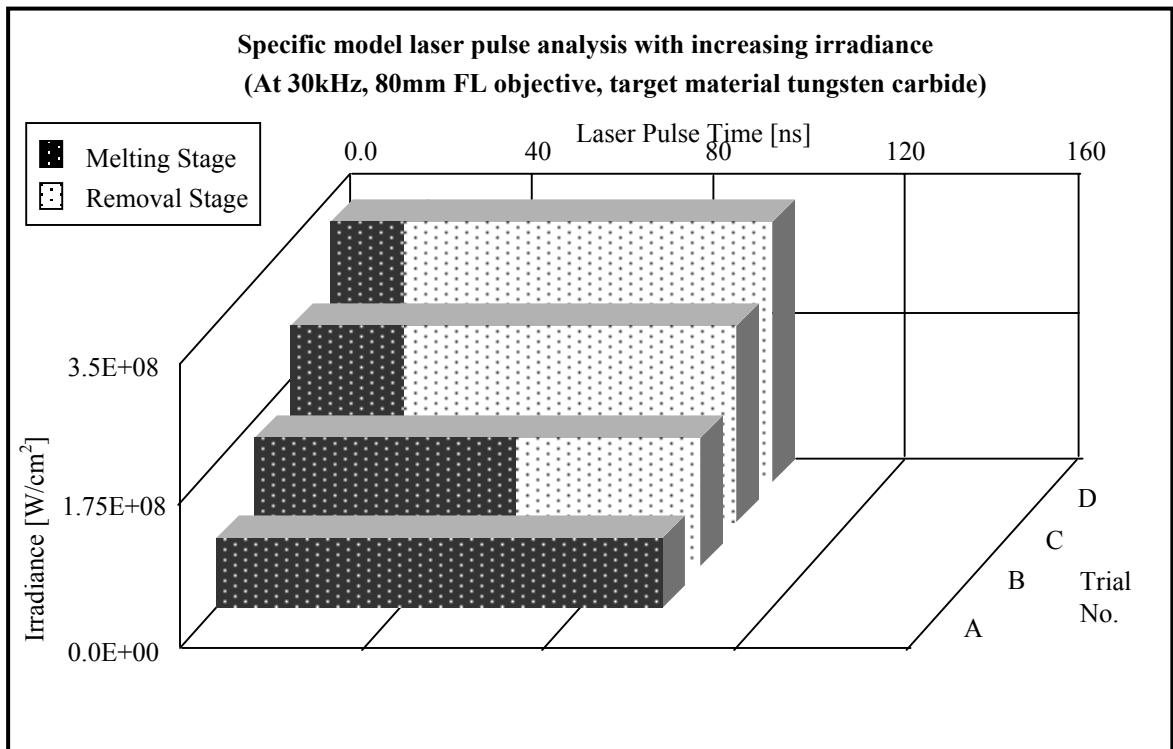


Figure 6 : Analysis of irradiance effects on Melting Stage for Test Case 3

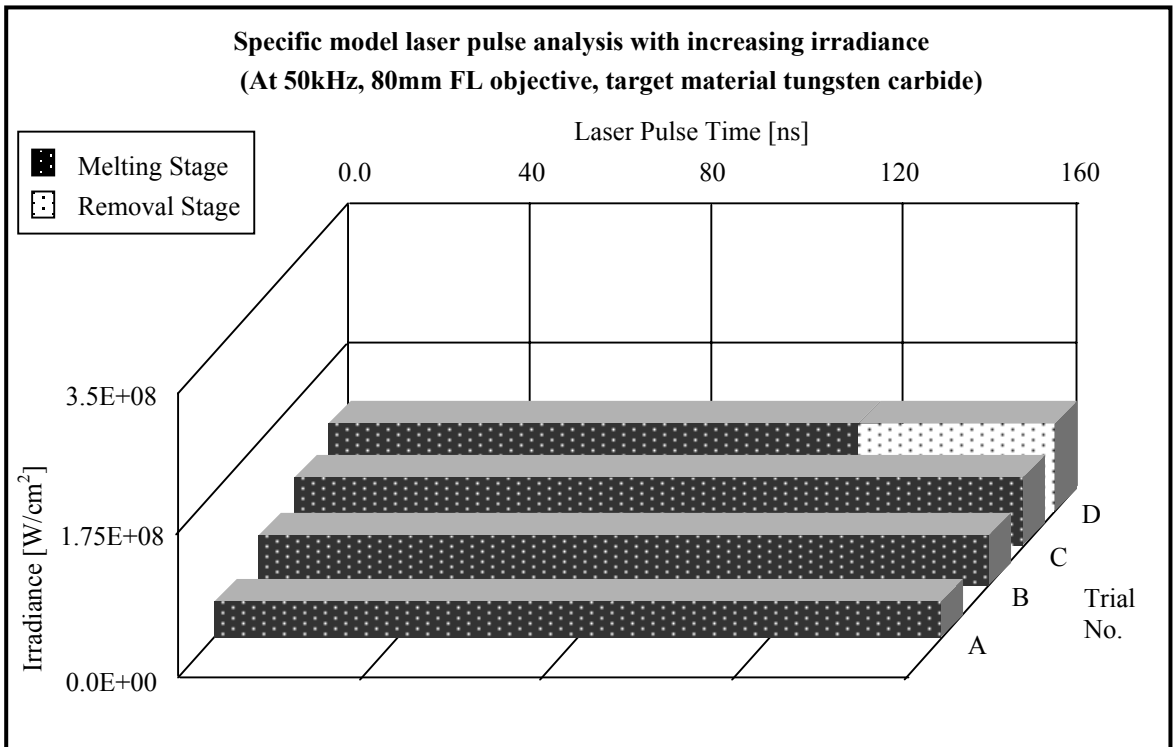


Figure 7 : Analysis of irradiance effects on Melting Stage for Test Case 4

### 3.4. Comparison of modelled and experimental results

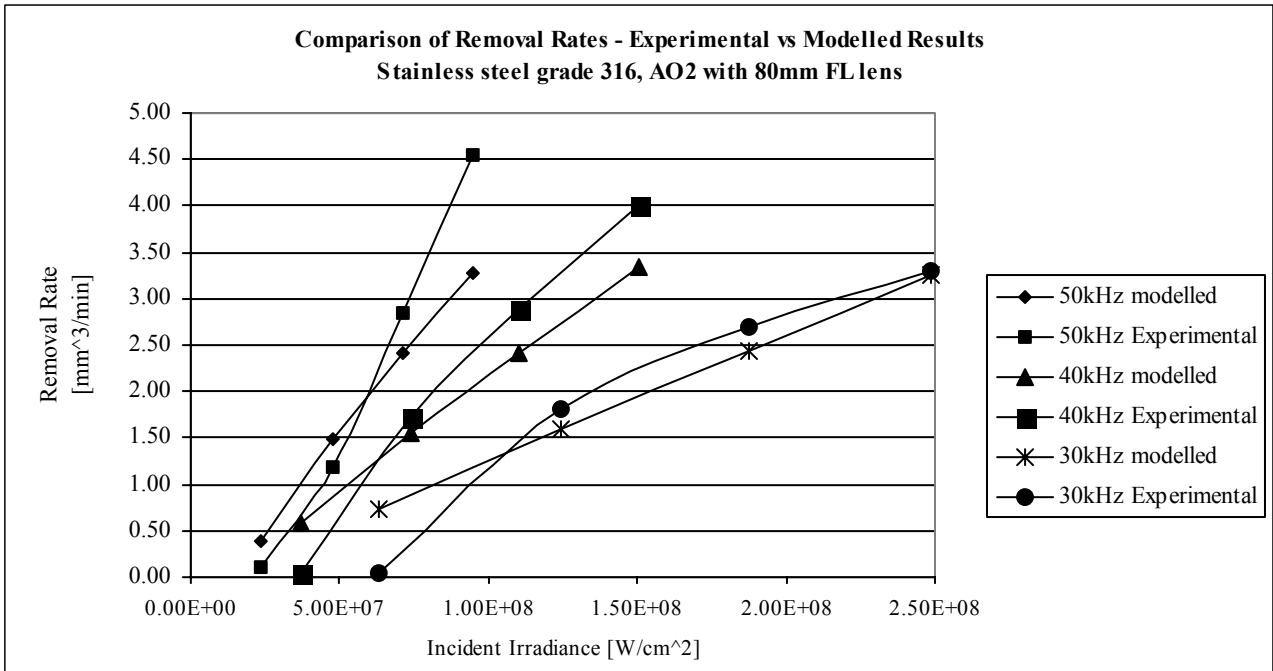


Figure 8 : Comparison of experimental and modelled removal rates for stainless steel.

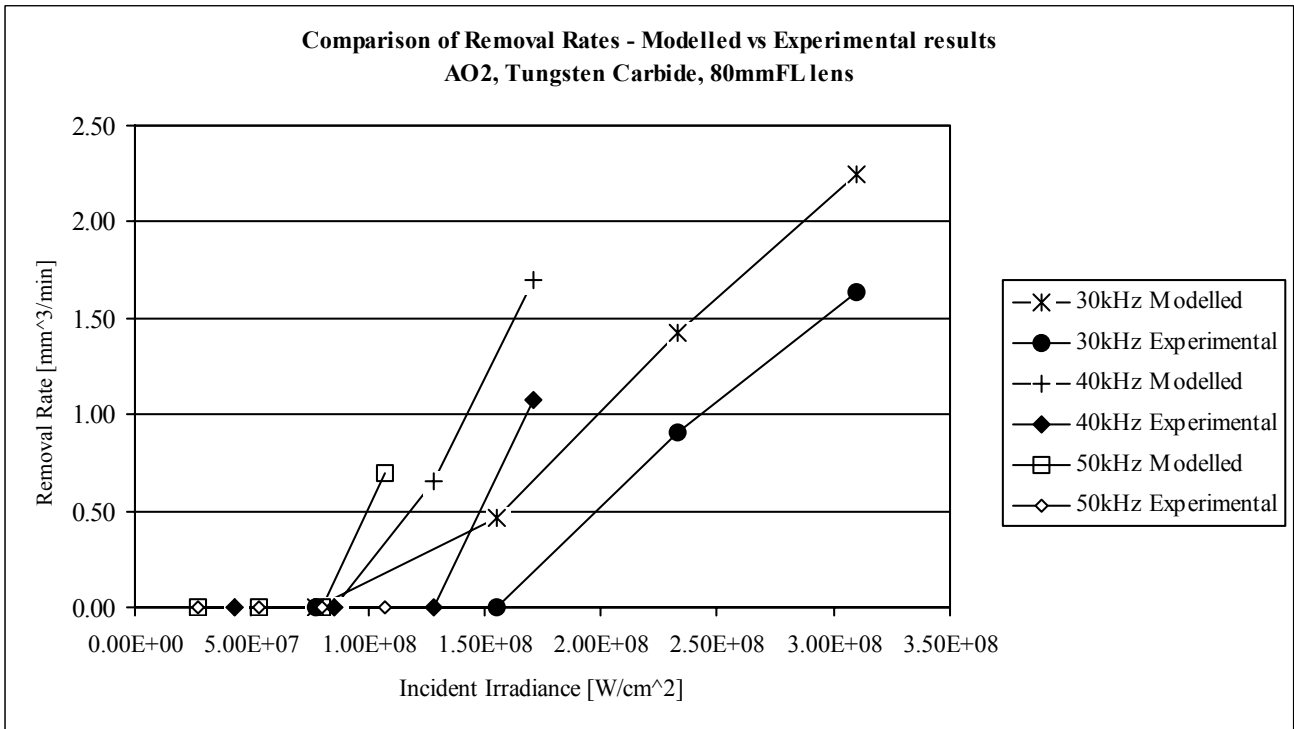


Figure 9 : Comparison of experimental and modelled removal rates for tungsten carbide

Figures 8 and 9 show the comparison between modelled and experimental work for stainless steel grade 316 and tungsten carbide. Figure 3 shows the laser parameters (laser repetition rate, pulse width and irradiance) used to obtain the results.

The modelled and experimental results for Test Case 1 were directly compared to generate a scaling factor for the model. This factor is a constant multiplier that is used to scale all removal rates calculated. Once obtained (using only Test Case 1) the scaling factor was then applied to all other modelled removal rate results.

Comparing modelled and experimental results at corresponding laser repetition rates for stainless steel, generally the results match each other quite closely – note the similarity of the gradients of lines of corresponding repetition rates. It can be seen that the gradient of the 30kHz experimental results curve starts to drop off at higher irradiances - this could be plasma blocking starting to have an effect.

Figure 8 also shows that at 50kHz the incident irradiance per pulse is lower than for 40kHz and 30kHz yet the modelled removal rate is comparable and the experimental removal rate is higher. This is explained in 2 ways :

- At 50kHz the pulse width is significantly longer but has a lower irradiance and it can be seen in Section 3.3 that the modelled volume removed by a single pulse at 50kHz is a little less than that at 30kHz. In addition, at 50kHz there are 66% more pulses, so whilst the removal per pulse can be lower the overall the removal rate can be higher. This is predicted in Section 3.3.
- Secondly it was noted during the experimental tests that molten debris was starting to be ejected from the target during some of the tests at higher irradiances. This is a less controlled removal regime than removal by vaporization. It can produce higher removal rates but with lower quality results - poor shape control, thicker recast layer and more surface debris, and is not considered in the model.

Figure 8 also shows that the maximum modelled removal rate for this study for all three repetition rates is almost the same – so which repetition rate is chosen in practise? All of the work in this study has used a Starlase AO2 laser operating at maximum power output which has provided the upper limit for the experimental irradiances. If this laser was used in practise it would be operated at 50kHz because it is furthest away from the LSA limit, and the experimental removal rates are slightly higher. However, if a more powerful laser was used (for instance a Starlase AO4) the same repetition rates could be used with higher irradiances. The modelled data in Figure 8 could be extended and projected at the given gradients to predict removal rates at these higher irradiances. As the irradiance is increased the LSA limit is approached ( $1.5 \times 10^8 \text{ W/cm}^2$ ) where useful removal begins to be limited by a plasma shield<sup>1,3</sup>. Since the 50kHz repetition rate operates at the lowest irradiance, it could be extended further than the lower repetition rates before reaching this limit. Therefore for stainless steel, 50kHz repetition rate has the potential to give the highest overall removal below the LSA limit.

Figure 9 shows the modelled and experimental results for tungsten carbide. It can be seen for the experimental results that as the laser repetition rate increases the removal rate decreases, and this is predicted by the modelled results as shown in Section 3.3. The model shows why the removal rate drops to zero at 50kHz repetition rate– the material does not reach its vaporization temperature, so there is no vaporization and therefore no removal. Only at lower repetition rates where the irradiance level is high enough to reach the vaporization temperature within the duration of the pulse is material removed.

### 3.5. Guidelines for Future Ablation Trials

Following the work done in this study, a set of guidelines have been developed that are intended to assist the characterisation of future laser ablation trials. They are as follows :

- *Minimum Pulse Irradiance.* For a specific pulse width generated by a DPSS laser and given material properties, the minimum irradiance that causes vaporization within the pulse duration can be calculated. This irradiance level should be lower than the LSA limit otherwise a longer pulse width should be

considered. Using a lower irradiance at this pulse width will have little effect on the material other than to melt it – there will be no removal of material.

- *Maximum Repetition Rate.* Using the Minimum Pulse Irradiance information in conjunction with the proposed focal spot size and the laser pulse output characteristics (similar to that shown in Figure 3), the maximum repetition rate can be identified that provides the required pulse irradiance. Lower repetition rates will also remove material provided that the irradiance remains below the LSA threshold, but generally the highest repetition rates will produce the highest ablation rates. This will help to select the most appropriate laser for practical trials.

#### 4. CONCLUSIONS

1. The latest generation of high power Q-switched DPSSLs are industrially robust tools capable of commercially enabling important industrial applications involved with milling stainless steels and tungsten carbide.
2. Within a defined set of assumptions the laser ablation process has been successfully modelled as a specific two stage process, and this model has been shown to correlate with experimental results for stainless steel grade 316 and tungsten carbide.
3. This model can be used to analyse many other materials provided that the correct material properties are available, such as Thermal Barrier Coatings and Nickel Superalloys.
4. A set of guidelines have been generated that can be used to aid future laser ablation trials.

#### Acknowledgements

The author would like to thank the Powerlase Applications Team for their assistance with this paper.

#### REFERENCES

1. J. F. Ready, *Industrial Applications of Lasers* (Second Edition), Chapter 12, Academic Press Ltd, London, 1997
2. W. M. Steen, *Laser Material Processing*, Chapter 3, Springer-Verlag, London, 1996
3. M. Henry, "Emerging Applications Enabled by High Power Nanosecond Pulsed Diode Pumped Solid State Lasers", ICALAO 2003 Conference Proceedings, LIA Vol. 95, October 2003.
4. P. Harrison, M Henry, I Henderson, Unpublished Results, Powerlase Ltd, Crawley, UK, 2001-2004
5. J. F. Ready, *LIA Handbook of Laser Materials Processing*, Chapter 5, Magnolia Publishing, 1<sup>st</sup> edition, 2001.
6. J. R. Untermahrer et al, "High peak power diode-pumped solid state lasers and industrial applications", CLEO 1998 Technical Digest, Vol 6, May 1998.
7. T.A. Mai et al, "Laser ablative micro-machining and it's applications for rapid fabrication of micro-fluidic components", ICALAO 2002 Conference Proceedings, LIA Vol. 94, October 2002.